ChemPubSoc Europe

DOI: 10.1002/chem.201701728

CHEMISTRY A European Journal Full Paper

Organometallic Chemistry |*Hot Paper*|

Self-Assembly of Di-N-Heterocyclic Carbene-Gold-Adorned Corannulenes on C_{60}

Carmen Mejuto,[a] Luis Escobar,[b] Gregorio Guisado-Barrios,[a] Pablo Ballester,[b, c] Dmitry Gusev,*[d] and Eduardo Peris*[a]

Abstract: The deprotonation of a corannulene-based bisazolium salt allowed the preparation of a corannulene-based NHC di-Au^{I} complex. The prepared di-Au^{I}-complex was tested in the recognition of fullerene-C_{60}, demonstrating good binding affinity in toluene solution, and producing a host–guest complex with 3:1 stoichiometry, as evidenced by a combination of NMR spectroscopy and ITC titrations. The experimental results are fully supported by DFT calculations. The binding of C_{60} with the di-Au^{I} complex in toluene solution is enthalpically and entropically favoured. Remarkably, the entropic term is the dominant parameter in the binding process. The good complementarity that exists between the concave shape of the corannulene-di-gold complex and the convex surface of the fullerene, together with the presence of *t*Bu groups and the AuCl fragment are key factors for the measured high affinity between host and guest. The obtained results indicate that fullerene may be acting as a template for the formation of a self-assembled aggregate involving up to three molecules of the di-Au^{I} complex.

Introduction

Shape and size complementarity are among the most important factors to be considered in the design of efficient molecular receptors. Since the discovery of fullerenes, the interaction of their curved, conjugated and convex surfaces with properly assembled polyaromatic systems has been a prominent area of research.[1] The design of efficient fullerene receptors is based on establishing suitable face-to-face contacts between (preferably) the concave faces of polyaromatic systems and the convex and conjugated surface of the former in order to establish efficient van der Waals intermolecular interactions. Some of the known fullerene receptors are suitable for the separation/extraction of certain fullerenes from complex mixtures or even from fullerene-containing carbon soot.[2] Bowl-shaped polyaromatic hydrocarbons, such as corannulene, which can now be prepared on the kilogram scale,[3] are among the best binding units to be incorporated in synthetic molecular receptors for fullerenes. This is mainly due to the shape complementarity that exists between the shallow concave cavity of the corannulene and the convex surfaces of the fullerenes.[4]

Although based on theoretical calculations the interaction of corannulene with C_{60} is energetically favourable in the gas phase,[5] and close contacts between the two binding partners are experimentally observed in the solid state,[6] to the best of our knowledge, there are no literature reports on the binding affinity for the two binding partners in solution. Probably the closest description of this type of interaction was reported by Yamada and co-workers who determined a low association constant ($19\ M^{-1}$) between a lithium ion encapsulated-[60]fullerene ($Li^{+}@C_{60}$) with corannulene.[7] The low binding affinities between C_{60} and corannulene in solution have been attributed to the dissolvation and entropic binding penalties that presumably are associated with the formation of a fullerene@corannulene inclusion complex in solution.[8] In order to circumvent these penalties, elaborate synthetic receptors combining two or more corannulene binding units were recently synthesized. These fullerene receptors, so-called "buckycatchers", showed remarkable affinities for fullerene binding in solution (representative examples of the synthetic receptors **A**–**C** are shown in Scheme 1).[9] Some receptors based on the modification of a single corannulene unit have also been reported (D–**E**, Scheme 1). The pentaindenocorannulene **D** displays a bowl-shaped curvature similar to that of corannulene, but features a larger surface area provided by the presence of five benzo-fingers, which are also responsible for the increase in the depth of the receptor's cavity.[5d,10] A recent study described

[a] *C. Mejuto, Dr. G. Guisado-Barrios, Prof. E. Peris*
Institute of Advanced Materials (INAM). Universitat Jaume I.
Av. Vicente Sos Baynat s/n. Castellón. 12071 (Spain)
E-mail: eperis@uji.es

[b] *L. Escobar, Prof. P. Ballester*
Institute of Chemical Research of Catalonia (ICIQ)
The Barcelona Institute of Science and Technology
Avgda. Països Catalans 16, 43007 Tarragona (Spain)

[c] *Prof. P. Ballester*
ICREA, Passeig Lluís Companys 23, 08010 Barcelona (Spain)

[d] *Prof. D. Gusev0000-0003-3302-356X*
Dept. of Chemistry and Biochemistry
Wilfrid Laurier University, Waterloo, Ontario N2L 3C5 (Canada)
E-mail: dgoussev@wlu.ca
Homepage: 0000-0003-3302-356X

Supporting information and the ORCID identification numbers for the authors of this article can be found under https://doi.org/10.1002/chem.201701728.

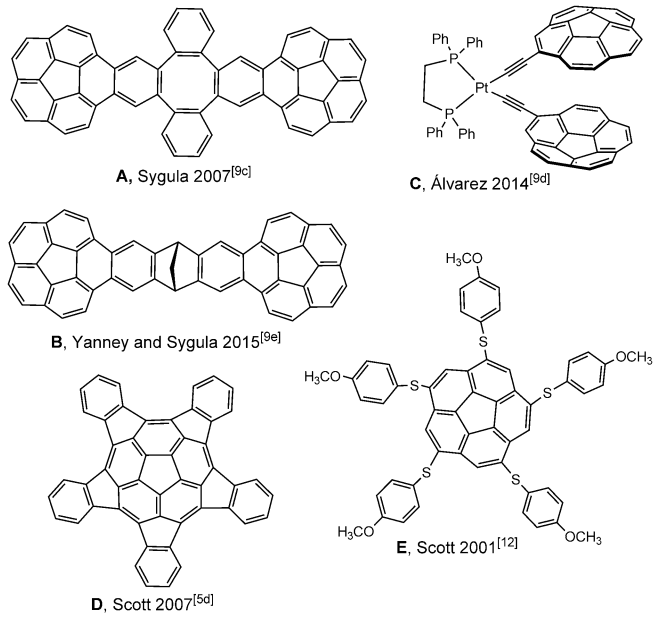

Scheme 1. Line-drawing structures of "buckycatchers" **A**–**C**, pentaindeocorannulene **D**, and corannulene derivative **E** featuring five geodesic electron-rich arms

the formation of 1:2 inclusion complexes, C_{60}@$\mathbf{D}_2$, between pentaindenocorannulene **D** and C_{60} both in solution and in the solid state. However, the binding constant values for the 1:1 and the 1:2 aggregates were not reported.[11] Significantly, the structure of the 1:2 complex, which was determined in the solid state, showed the C_{60} bound to the concave face of a $\mathbf{D}_2$ dimer rather than the C_{60} being sandwiched between two $\mathbf{D}_2$ units. Related to these findings, some years ago corannulene derivatives possessing geodesic electron-rich arms (**E**) were described to form 1:1 complexes with C_{60} in toluene solution. The association constant values determined for the formed 1:1 complexes were in the range of 200–400 M^{-1}.[12] This finding was interpreted as a consequence of the establishment of enhanced attractive noncovalent interactions between the electronically complementary surfaces of the functionalized corannulene and the C_{60} in the donor–acceptor complex. Some receptors bearing three tethered corannulene functionalities were been reported, but they did not exhibit any affinity enhancement toward fullerene as compared to bi-corannulene analogues, suggesting that not all three corannulene fragments embrace fullerene at the same time.[9f,h] This is probably due to the geometry restrictions imposed by the tether, which does not allow an optimized distribution of the corannulene fragments around the surface of the fullerene.

During the last few years we have developed a series of di- and tri-N-heterocyclic carbene ligands connected by planar fused polyaromatic linkers.[13] In the course of our research, we found that this type of ligands afforded unique catalytic properties to the resulting organometallic complexes, which we ascribed to supramolecular effects.[14] In pursuit of a novel polyaromatic linker that could endow with new properties to the resulting bis-NHC ligands, we turned our attention to corannulene owing to its unique electronic and topologic features. We envisaged that a corannulene derivative bearing bis-NHC ligands in its periphery could be applied not only in catalysis but also in supramolecular binding studies with fullerenes.

Results and Discussion

The synthetic procedures used for the preparation of the compounds described in this work are summarized in Scheme 2. The tetraamination of tetrabromocorannulene **1**[3] was performed by using *tert*-butylamine in the presence of a palladium catalyst, and afforded the tetraamino corannulene **2** in an almost quantitative yield (97%). The bis-annulation of **2** was performed by treating it with tributyl orthoformate. The reaction afforded the corannulene-bisazolium salt **3** in 66% yield. The ^{1}H and ^{13}C NMR spectra of **3** were consistent with the C_s symmetry of the molecule (see the Supporting Information). The ^{1}H NMR ([D_6]acetone) spectrum showed a singlet at 9.55 ppm, which was assigned to the NCHN hydrogen atom. This proton signal is diagnostic of the formation of azolium salts.

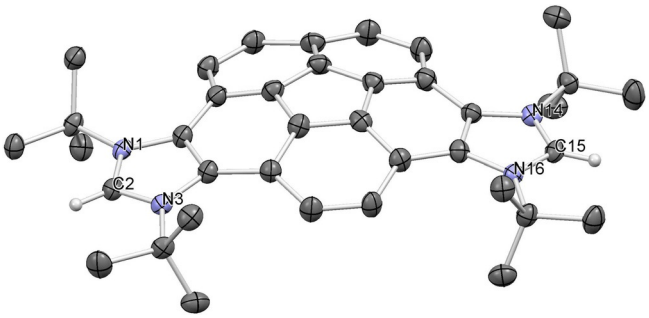

Figure 1. X-ray structure of **3**. Thermal ellipsoids set at 50% probability. Hydrogen atoms (except hydrogens at NCHN), counter-anions ($2PF_6^-$) and solvent (1,2-dichloroethane) are omitted for clarity. Selected bond distances [Å] and angles [°]: N(1)-C(2) 1.319(3), N(3)-C(2) 1.326(3), N(14)-C(15) 1.331(3), N(16)-N(15)1.323(3), N(1)-C(2)-N(3) 112.0(2), N(16)-C(15)-N(14) 111.5(2).

The molecular structure of **3** was further confirmed by single crystal X-ray diffraction. The structure of **3** is shown in Figure 1, and reveals the presence of the two imidazolium rings bridged by the corannulene spacer. The bowl-shape of the corannulene induces a dihedral angle between the two planes defined by the azole units of 15.6°, therefore the two imidazolium fragments are not co-planar. The *tert*-butyl substituents of the nitrogen atoms adopt the less hindered conformation by pointing one of their methyl groups toward a putative coordinated metal, assuming that an N-heterocyclic carbene complex could be formed. The X-ray structure of **3** allowed us to estimate that if a dimetallic di-NHC complex was formed, the metal–metal distance would be approximately 11.9 Å.

Deprotonation of the bisazolium salt **3** to produce the corresponding bis-N-heterocyclic carbene ligand **4** was performed in [D_6]benzene by using sodium bis(dimethylsilyl)amide (NaHMDS) and a catalytic amount of sodium *tert*-butoxide. The resulting solution of **4** was analysed by NMR spectroscopy (see

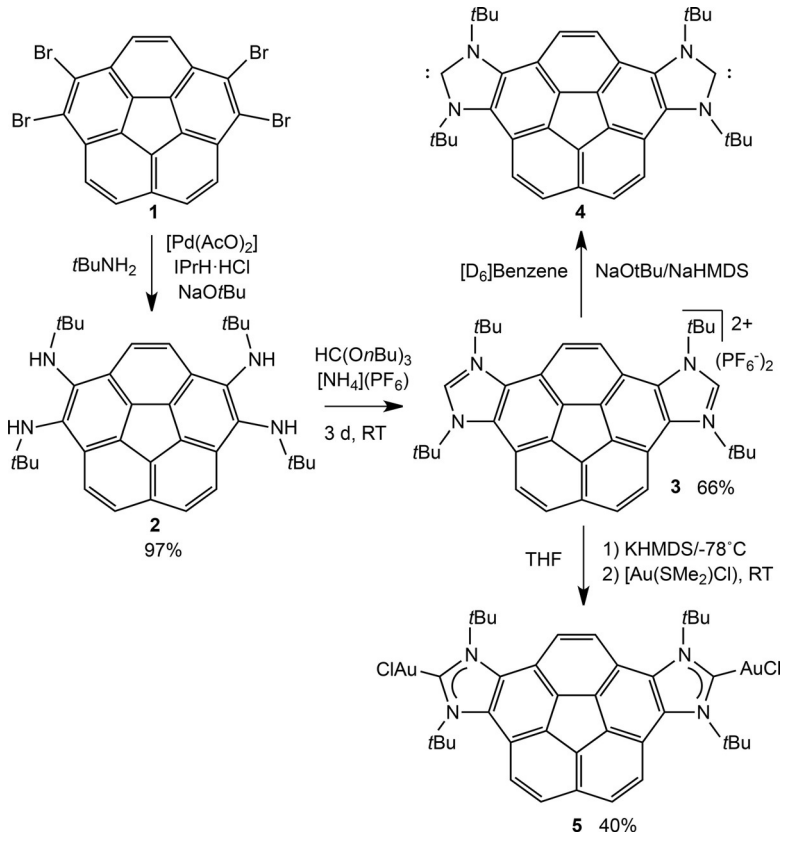

Scheme 2. Synthesis of corannulene derivatives **2**–**5**.

the Supporting Information). The ^{13}C NMR spectrum of the solution displayed the diagnostic signal of the carbene carbon at 219.9 ppm. Compound **4** was stable in benzene for several days. The reaction of **3** with [AuCl(SMe_2)] in THF, in the presence of KHMDS, afforded the bis-NHC di-gold(I) complex **5**, in a moderate yield (40%). The di-gold complex **5** was characterized by a complete set of high-resolution spectra and elemental analysis (see the Supporting Information). The ^{13}C NMR spectrum of complex **5** displayed a signal at 178.7 ppm, assigned to the carbene carbon. The mass spectrum (ESI-TOF-MS) revealed two main ion peaks at *m/z* ratios of 787.3 and 1041.3, that were assigned to $[M-AuCl+H]^+$ and $[M+Na]^+$ species, respectively.

We probed the interaction of the bowl-shaped gold complex **5** with fullerene using ^1H NMR spectroscopy. The ^1H NMR spectrum of **5** in [D_8]toluene showed sharp and well-defined proton signals. The H_a proton resonates as a singlet at 8.08 ppm. On the other hand, protons H_b and H_c appear as doublets at 8.08 and 7.56 ppm, respectively (see Figure 2 for ^1H assignations). We observed that the incremental addition of C_{60} (guest) to a millimolar solution of **5** (host) induced a downfield shift of the corannulene proton signals of **5**, as can be observed from the series of spectra shown in Figure 2. The addition of 8 equivalents of C_{60} produced a downfield shift of 0.4 ppm of the signal due to the corannulene hydrogen labelled as H_a (Figure 2. The assignation of the signals can be found in the Supporting Information). The signals labelled as H_b, H_c and the ones due to the protons of the *tert*-butyl group also experienced a downfield shift, although to a lower extent than that observed for H_a. The chemical shift changes experienced by the proton resonances of the corannulene unit in **5** are indicative of a binding process with C_{60} that showed fast kinetics on the NMR timescale. We assumed that the bimetallic complex **5** interacts with C_{60} through π–π donor–acceptor interactions. The assessment of the associations was performed by simultaneously adjusting the chemical shift changes experienced by the signals of H_a, H_b and H_c, to the corresponding binding models (1:1, 1:2 and 1:3, related to C_{60}:**5**).[15] The fit for the formation of a 1:1 complex returned a binding constant value of $K_{11} = 2.982(\pm 2)\ M^{-1}$ (error taken from the statistical fit) for the formation of a C_{60}@**5** complex. Not surprisingly, the experimental data obtained in the titration displayed statistically significant improvements of the fit when switching from 1:1 to 2:1 and finally to 3:1 models, as concluded by the F-test statistical analysis (see the Supporting Information for full details about the statistical analysis of the fitting of all three binding models). The fittings were performed assuming that the microscopic binding constants for the stepwise binding steps leading to C_{60}@$\mathbf{5}_2$ and C_{60}@$\mathbf{5}_3$ were identical. The fits returned microscopic binding constant values that were coincident with the one determined for the exclusive formation of the 1:1 complex $K_a(C_{60}@\mathbf{5}) = 2.9\times10^3\ M^{-1}$. However, the fit to a 3:1 binding model gave a very good statistical fitting, we considered that the analyses of the titration data did not provide unambiguous evidences for the formation of a complex having this stoichiometry. The monotonic shift experienced by the an-

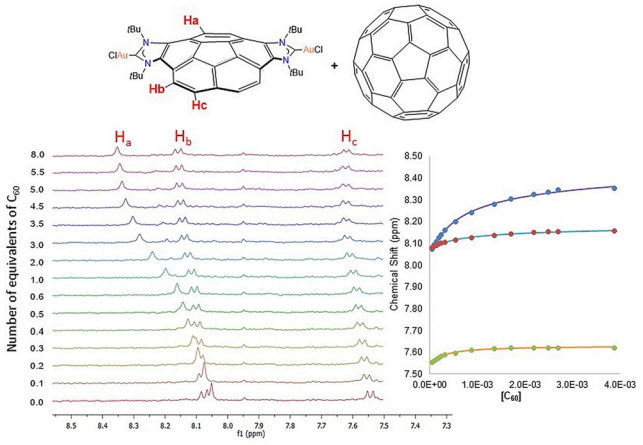

Figure 2. Selected regions of the ^{1}H NMR (500 MHz, [D_8]toluene, 298 K) spectra acquired during the titration of **5** with incremental amounts of C_{60}. The concentration of **5** was maintained constant (0.5 mM) throughout the titration. The binding isotherm is shown below.

alysed proton signals of corannulene derivative **5** upon binding C_{60} was not suitable to distinguish between the two possible theoretical binding models by relying only on the goodness of the fit. Taken together, these results indicate that: a) corannulene **5** interacts with C_{60} in solution at millimolar concentration; b) the chemical exchange between free and the bound **5** is fast on the NMR timescale, c) the binding constant for the interaction of one unit of **5** with C_{60} is on the order of $10^3\,M^{-1}$, and d) complexes of larger stoichiometry than the simple 1:1 C_{60}@**5** are apparently formed in the investigated range of millimolar concentrations.

We were also interested in studying if **5** could be used as receptor for planar polyaromatic hydrocarbons. As a model we used coronene for our binding studies. The addition of incremental amounts of coronene to a millimolar solution of host **5** in [D_8]toluene produced chemical shift changes in all its aromatic proton signals. The signals of the H_b and H_c protons experienced a downfield shift whereas the signal of the proton H_a moved upfield. The chemical shift changes experienced by all three signals (H_a, H_b and H_c) were analysed by using a 1:1 binding model. The fit returned an association constant value of $K_{11}=2.1(\pm0.2)\times10^2\,M^{-1}$ for the formation of the coronene@**5** complex. The binding constant value is one order of magnitude smaller than the one determined for C_{60}@**5** complex. We assigned this reduction of binding affinity to the reduced shape complementarity between the binding partners. On the other hand, the obtained results serve to illustrate that complex **5** can also be used for the recognition of large planar polycyclic aromatic hydrocarbons like coronene.

In order to shed more light on the binding affinity of **5** with C_{60}, we carried out UV/Vis and fluorescence titrations. These spectroscopic techniques allowed the use of **5** at lower concentrations than those required for ^{1}H NMR titrations. By working at lower concentrations of **5** we expected to disfavour the formation of the aggregates with higher stoichiometry (e.g., 1:2 and 1:3 complexes), and therefore, gaining additional information on the thermodynamic stability of the 1:1 inclusion complex. The UV/Vis spectroscopic titration of **5** with incremental amounts of C_{60} did not show any noticeable changes in the absorption spectrum of the former. Conversely, the emission spectra of **5** changed significantly by the addition of increasing concentrations of C_{60}. Figure 3 shows the changes

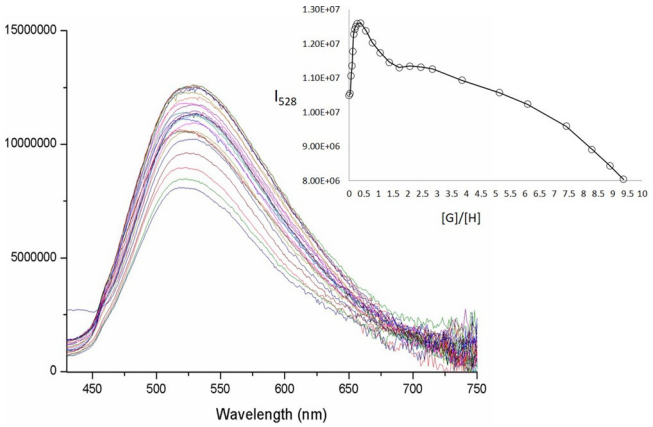

Figure 3. Fluorescence spectra acquired during the titration of **5** (1.55×10^{-5} M) with C_{60} (2×10^{-4} M) in toluene at 298 K ($\lambda_{ex}=403$ nm). The inset plot represents ΔI_{528} against the number of added equivalents of C_{60}.

observed in the emission spectra of **5** (1.55×10^{-5} M) in toluene upon incremental addition of fullerene. The fluorescence titration showed two phases. In the initial phase, the incremental addition of C_{60} provoked an increase in the intensity of the emission band of **5** centred at 528 nm. However, when the ratio of [C_{60}]/[**5**] > 0.4, the intensity of the emission band started to decrease. We interpreted the quenching effect of the second phase of the titration as a consequence of the increase of absorption at the excitation wavelength that was caused by the incremental C_{60} addition (inner filter effect). Consequently, the emission titration data are not suitable for mathematical analysis using a theoretical binding model. However, they do serve to support the interaction of **5** with C_{60} even at micromolar concentration that is responsible for the increase of emission of the host in the initial phase of the titration.

We thought that isothermal titration calorimetry (ITC) experiments should help us to obtain additional experimental information on the interaction of complex **5** with C_{60}. ITC is a thermodynamic technique that directly measures the heat released or absorbed upon sequential and incremental addition of a solution of one compound to another solution of the same solvent containing a different compound. Due to the reduced solubility of the two binding partners, the titrant (C_{60}) and the titrand (**5**) concentrations used in the ITC experiment were suboptimal considering the tentative binding affinity for C_{60} with **5** on the order of $10^3\,M^{-1}$, determined using the ^{1}H NMR titrations (vide supra). The ITC experiment was performed by incremental addition of a toluene solution of C_{60} (3.8 mM) to a toluene solution of **5** (0.6 mM) placed in the cell. The initial injections produced the observation of significant evolved heat, indicative of an exothermic process. The experimental binding isotherm was analysed by using the "one set of sites"

theoretical binding model implemented in the Microcal software.[16] We obtained the best fit for the model that assumed three equivalent binding sites and the formation of a 1:3 complex C_{60}@**5**$_3$ (Figure 4). This finding suggests that C_{60} interacts

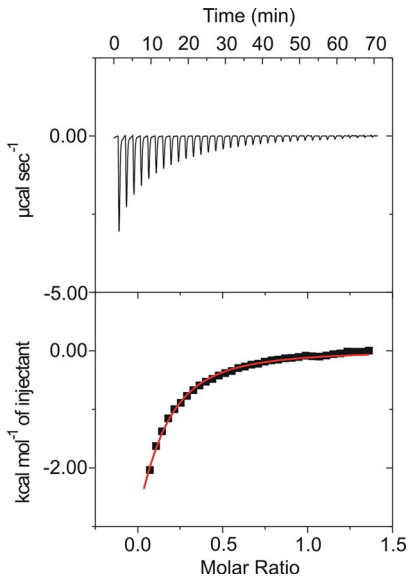

Figure 4. Top: heat versus time plot of the ITC experiment of **5** (0.6 mM) with incremental additions of C_{60} (3.8 mM), in toluene at 298 K. Bottom: the best fit of the integrated heats to the theoretical binding isotherm obtained assuming three ($N=3$) equivalent binding sites in C_{60}@**5**$_3$. The resulting thermodynamic data (K, ΔH, and ΔS) are per mole of **5**.

with **5** forming consecutive 1:1, 1:2, and 1:3 inclusion complexes, in agreement with the conclusions derived from the ^{1}H NMR titration experiments. The fit of the experimental ITC data to the theoretical binding model also allowed the determination of an average value of the binding constant of C_{60} with **5** and the average enthalpy of binding (ΔH) of the process. The free energy (ΔG) and the entropy (ΔS) terms were calculated from the experimental thermodynamic parameters, K and ΔH. The average stability constant K for the formation of C_{60}@**5**$_3$ was $7.1(\pm 0.7)\times 10^3$ per mole of **5**, in agreement with the value determined by using ^{1}H NMR titrations. The average enthalpy change per step and per mol of **5** leading to the formation of C_{60}@**5**$_3$ was $\Delta H = -0.67(\pm 0.07)$ kcal mol^{-1}. Remarkably, the calculated entropic term, $T\Delta S$, was positive and had a value of $4.6(\pm 0.5)$ kcal mol^{-1}. Therefore, entropy contributed significantly to the free binding energy that in turn was calculated to be $-5.3(\pm 0.5)$ kcal mol^{-1}. All together, these results indicate that in toluene solution both enthalpy and entropy terms favour stepwise formation of the product C_{60}@**5**$_3$ complex and its 1:1 and 1:2 precursors. This result contradicts the established paradigm stating that the binding of C_{60} with receptors containing a single corannulene unit must be entropically disfavoured.[8] On the contrary, our finding is in line with the recent reports of favourable entropic terms in the complexation of C_{60} with receptors containing more than one corannulene binding unit.[9a] We rationalize the observed favourable entropy for binding through the assumption that solvation/desolvation processes of the free and bound components must play an important role in the binding process.

We performed a series of DFT calculations to determine the structures and binding energies of the complexes produced by the interaction of **5** with C_{60}. Studying such systems is challenging from the computational point of view because bonding between **5** and C_{60} in C_{60}@**5**$_n$ is governed by noncovalent interactions and the ultimate product C_{60}@**5**$_3$ is excessively large: $C_{174}H_{126}N_{12}Cl_6Au_6$. Understandably, calculated DFT energies of supramolecular systems in solution should be treated with caution, thus, the principal objective of this study was to establish any trends upon the formation of C_{60}@**5**$_n$ with $n=1$–3. To gauge the accuracy of the calculations, we employed four local DFT methods: M06L/Def2SVP//M06L/Def2QZVP (method M1), M06L-D3/Def2SVP//M06L-D3/Def2QZVP (M2), B97D3/Def2SVP//B97D3/Def2QZVP (M3), B97D/Def2SVP//B97D/Def2QZVP (M4). A limited amount of computational work, for comparison, was also carried out at the ωB97XD/Def2SVP//ωB97XD/Def2QZVP (M5) level. The Def2QZVP basis set was used for Au during the geometry optimizations, together with the corresponding effective core potential (def2) available in Gaussian 09.[17] The polarizable continuum model (IEFPCM) was employed in all calculations in toluene, with the radii and non-electrostatic terms of Truhlar and co-workers' SMD solvation model. Along with **5**, we calculated the smaller version of this complex possessing all N–CH_3 groups (**5**′). Ultimately, the geometries of C_{60}@**5**′, C_{60}@**5**′$_2$, and C_{60}@**5**′$_3$ could be optimized, whereas only C_{60}@**5** and C_{60}@**5**$_2$ were computationally accessible. As a technical note, the B97D3 geometry optimizations of this work systematically produced structures with at least one "negative" vibrational frequency, whereas this problem was not encountered with the other methods M1, M2, M4, or M5.

It is appropriate to start the review of the DFT results by analysing the structures of **5**′ and **5** in Figure 5. These bowl-shaped molecules share a common corannulene core, however **5**′ is distinctly more "shallow" compared to **5**. With respect to the centroid X of the corannulene, the Cl–X–Cl angle in **5**′ is more open compared to **5**: 134.0° versus 115.5°, respectively. The increased bending of the Au–Cl fragments in **5** is caused by the *tert*-Bu groups adopting an orientation with one C–Me bond perpendicular to the carbene fragment. Thus, counterintuitively, the *bulkier* complex **5** appears to have a more appropriate shape (concave curvature) to complement the convex form of the fullerene surface upon complex formation.

Next, we addressed the structure of **5** in toluene solution. Establishing the nature of the ground-state of **5** in this solvent is a considerable challenge and can be assessed only to a certain degree. Based on the experimental *positive* entropy determined for the formation of the inclusion complex C_{60}@**5**$_3$, it is appropriate to view the complexation process as proceeding with displacement of toluene from the bowl-shaped **5**. The cavity of **5** is large enough to fit in two solvent molecules. A computational search for the best accommodation of toluene in **5** returned the structure of Figure 6 where the solvent molecules adopt an "*anti*" orientation, that is, with the methyl groups facing the opposite sides of **5**. The toluene molecules are engaged in multiple interactions over and at the periphery

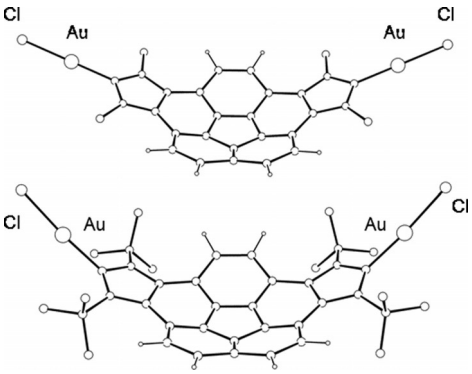

Figure 5. Geometries of **5′** (above) and **5** (below) calculated by using the ωB97XD (M5) method.

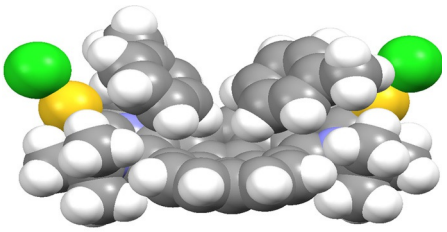

5′@toluene$_2$	**5**@toluene$_2$
-5.7 (M1)	-6.9 (M1)
-8.1 (M2)	-9.9 (M2)
-9.6 (M3)	-9.4 (M3)
-10.1 (M5)	-10.8 (M5)
-11.4 (M4)	-12.1 (M4)

Figure 6. The space-filling view of toluene$_2$@**5**. The enthalpies [kcal] of toluene binding to **5** and **5′** are in toluene at 298 K, per mole of toluene, calculated with methods M1–M5.

of the carbene fragments, involving contacts to the gold and chloride, as well as several hydrogen and carbon atoms. With respect to the centroid X of the corannulene, the Cl–X–Cl angle is contracted in toluene$_2$@**5** to 110.6° from 115.5° in the structure of **5** in Figure 5. The calculated enthalpy of formation of toluene$_2$@**5** varies from about −7 to −12 kcal per mole of toluene, depending on the functional used. The B97D (method M4) and ωB97XD (M5) calculations gave the most tightly bonded structures. The trend of the methods of this work predicting increasingly negative binding enthalpies in the order M1 < M2 < M3 < M5 < M4 will be seen again in the following discussion of C$_{60}$@**5**$_n$ and C$_{60}$@**5′**$_n$.

The results of DFT calculations on C$_{60}$@**5′**$_n$ (n = 1–3) and C$_{60}$@**5**$_n$ (n = 1, 2) are summarized in Figures 7, Figure 8 and Figure 9. Before discussing these, it is worth recalling that the π–π stacking interaction between C$_{60}$ and corannulene is relatively weak; for example, the prototypical C$_{60}$@corannulene inclusion complex has not been detected in solution.[7] This points at the gold carbene fragments of **5** as the structural motifs to which C$_{60}$@**5**$_3$ significantly owns its stability.

The results of Figures 7–9 present several salient points. First, the formation of C$_{60}$@**5** is more favourable compared to C$_{60}$@**5′**. This result can be attributed to the more extended and deeper cavity of **5** verses **5′** and the better shape-size complementarity of **5** and C$_{60}$ and thus the stronger dispersion attractive forces that stabilize the C$_{60}$@**5** complex. It is worth noting that the trend in the thermodynamic stability of the complexes increases in the order C$_{60}$@**5** < C$_{60}$@**5**$_2$ and C$_{60}$@**5′** < C$_{60}$@**5′**$_2$ < C$_{60}$@**5′**$_3$. In short, the products become markedly more stable as the number of complexed di-gold carbene **5** molecules increases. The molecules of **5** are docked in C$_{60}$@**5**$_2$ (Figure 9) by establishing multiple Cl···H contacts ranging from 2.75 to 3.74 Å and the additional H···H contacts at 2.51–2.65 Å. Overall, the structure of C$_{60}$@**5**$_2$ resembles a clamshell with

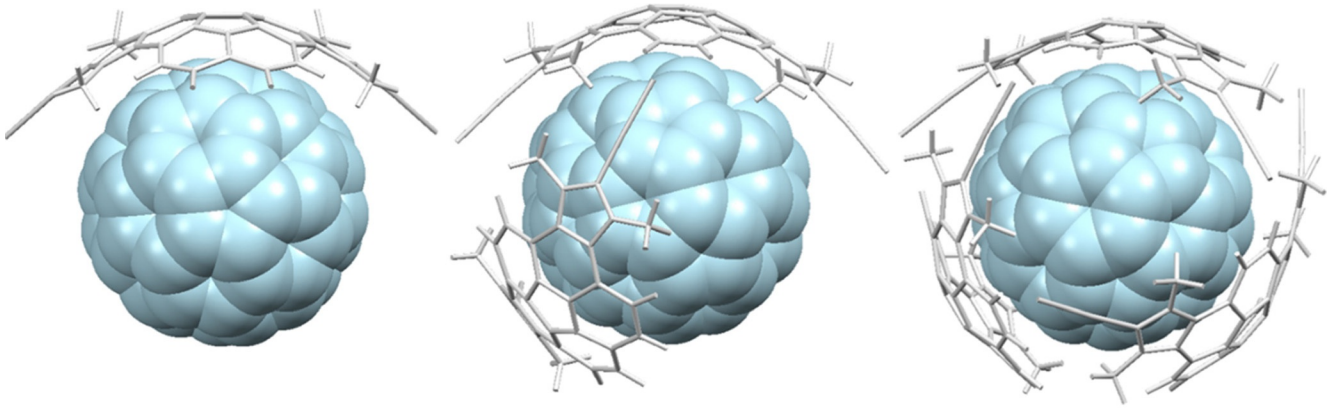

C$_{60}$@**5′**		C$_{60}$@**5′**$_2$		C$_{60}$@**5′**$_3$	
	ΔH (ΔS)		ΔH (ΔS)		ΔH (ΔS)
M1:	4.3 (27)	M1:	0.6 (24)	M1:	-2.6 (19)
M2:	2.5 (28)	M2:	-2.1 (21)	M2:	-6.2 (18)
M3:	2.2 (18)	M3:	-3.6 (20)	M3:	-7.7 (18)
M5:	1.4 (14)	M4:	-8.3 (19)	M4:	-12.8 (16)
M4:	-0.2 (21)				

Figure 7. Optimized geometries of C$_{60}$@**5′**$_n$ (n = 1–3). The enthalpies [kcal mol^{-1}] and entropies [cal K^{-1} mol^{-1}] of formation are in toluene at 298 K, per mole of toluene$_2$@**5**, calculated with methods M1–M5.

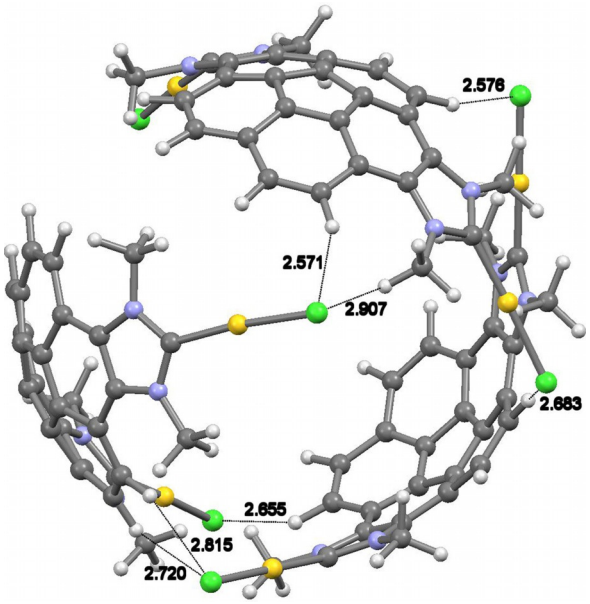

Figure 8. Optimized geometries of C_{60}@**5**′$_3$ showing some intermolecular Cl···H interactions. C_{60} was removed from the structure for clarity. Distances are in Å.

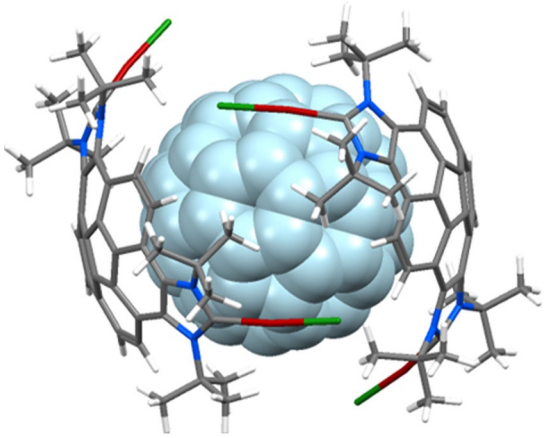

C_{60}@$\mathbf{5}_1$

	ΔH	(ΔS)
M1:	3.8	(19)
M2:	1.1	(16)
M3:	-1.2	(21)
M4:	-4.4	(22)

C_{60}@$\mathbf{5}_2$

	ΔH	(ΔS)
M1:	-2.2	(17)
M2:	-6.4	(17)
M3:	-7.4	(22)
M4:	-11.8	(19)

Figure 9. The optimized geometry of C_{60}@$\mathbf{5}_2$. The enthalpies [kcal mol^{-1}] and entropies [cal K^{-1} mol^{-1}] of formation of C_{60}@**5** and C_{60}@$\mathbf{5}_2$ are in toluene at 298 K, per mole of toluene$_2$@**5**, calculated with methods M1–M4.

a flexible joint. There is also a certain structural similarity between C_{60}@$\mathbf{5}_2$ and the "buckycatchers" developed by Sygula and co-workers[8] The structure of C_{60}@**5**′$_3$ has five of the six chlorides engaged in close Cl···H contacts (Figure 8), thus adding further stabilization to the complex with three bis-carbenes forming a beautifully docked molecular "puzzle" templated on C_{60}.

It is instructive to compare the DFT results of Figures 7 and 8 with the experimental values of Figure 5 ($\Delta H = -0.7$ kcal mol^{-1}, $\Delta S = 15$ cal K^{-1}·mol^{-1}, $\Delta G = -5.3$ kcal mol^{-1}). The best matching DFT values were obtained by using the M06L method M1. At this level of theory, the free energy of formation of C_{60}@**5**′$_3$ is -8.2 kcal mol^{-1}. C_{60}@$\mathbf{5}_3$ could not be calculated, however, its free energy of formation can be estimated by applying the energy difference between C_{60}@**5**′$_3$ and C_{60}@**5**′$_2$ ($\Delta G = -1.7$ kcal mol^{-1}) toward the energy of formation of C_{60}@$\mathbf{5}_2$ ($\Delta G = -7.2$ kcal mol^{-1}). This gives the estimated $\Delta G \leq -8.9$ kcal mol^{-1} for C_{60}@$\mathbf{5}_3$, suggesting somewhat tighter bonding in DFT calculations versus the experiment. The entropy change upon the formation of C_{60}@$\mathbf{5}_3$ should be $\Delta S \leq 17$ cal K^{-1} mol^{-1}, in close agreement with the experiment.

Conclusions

In summary, the deprotonation of a corannulene-based bisazolium salt allowed us to isolate and characterize a free corannulene-bis-imidazolylidene. This bis-NHC molecule was coordinated to gold, affording the corresponding corannulene-based NHC complex **5**. This organometallic complex was investigated as a receptor for the recognition of fullerene-C_{60}, where it showed a good binding affinity in toluene solution, and produced guest–host complexes of stoichiometries up to 1:3. This binding behaviour was evidenced by the combination of NMR and ITC titrations. The importance of the shape-complementarity between fullerene and the corannulene complex **5** is also illustrated by the much lower affinity showed by the organometallic complex in the recognition of a molecule having a flat-polyaromatic surface such as coronene. The results described here constitute a rare example of a synthetic molecular receptor containing a single corannulene binding motif displaying a strong interaction with fullerene-C_{60} in toluene solution. It is also important to mention that the magnitude of the average binding constant determined for **5** with C_{60} is on the same order of affinity as those reported for the more elaborated multitopic receptors that incorporate two or more corannulene binding units. In our case, the presence of the Au–Cl fragments and the *tert*-butyl groups of the di-NHC ligand substituents plays an important role in the stabilization of the product host–guest complexes. DFT calculations revealed how the presence of the *t*Bu groups in **5** facilitates the adaptation of the shape of the corannulene core to the fullerene surface. In turn, this shape complementary is responsible for an increase of their binding affinity. The Au–Cl fragments in the C_{60}@$\mathbf{5}_3$ complex allow close Cl···H intermolecular contacts, therefore suggesting a degree of cooperativity in the association of successive molecules of **5** to fullerene. An interesting point is that this result suggests that fullerene may be acting here as a template for the formation of a docked structure formed by the association of three molecules of **5**. Consequently and in view of these findings, the consideration of **5** being the host and fullerene being the guest could be switched. The change of roles is also in agreement with the general consensus in host–guest chemistry stating that the host–receptor may possess multiple binding sites.

Acknowledgements

We are very thankful to Professor Jay Siegel (University of Zurich/Tianjin University) for providing us with 1,2,5,6-tetrabromocorannulene, without which this work would not have been possible. We gratefully acknowledge financial support from MINECO of Spain (CTQ2014-51999-P) and the Universitat Jaume I (P11B2014-02). We are grateful to the Serveis Centrals d'Instrumentació Científica (SCIC) of the Universitat Jaume I for providing with spectroscopic facilities. We would also like to thank the MINECO of Spain for a fellowship (C.M.), MECD of Spain for a FPU fellowship (L.E.; FPU14/01016) and for a Juan de la Cierva grant (G.G.B.; IJCI-2015-23407).

Conflict of interest

The authors declare no conflict of interest.

Keywords: corannulene · fullerenes · gold · host–guest chemistry · N-heterocyclic carbene

[1] F. Diederich, M. Gomez-Lopez, *Chem. Soc. Rev.* **1999**, *28*, 263 – 277.
[2] a) D. Canevet, M. Gallego, H. Isla, A. de Juan, E. M. Perez, N. Martin, *J. Am. Chem. Soc.* **2011**, *133*, 3184 – 3190; b) Y. Shoji, K. Tashiro, T. Aida, *J. Am. Chem. Soc.* **2010**, *132*, 5928 – 5929; c) E. Huerta, G. A. Metselaar, A. Fragoso, E. Santos, C. Bo, J. de Mendoza, *Angew. Chem. Int. Ed.* **2007**, *46*, 202 – 205; *Angew. Chem.* **2007**, *119*, 206 – 209; d) E. Huerta, E. Cequier, J. de Mendoza, *Chem. Commun.* **2007**, 5016 – 5018.
[3] A. M. Butterfield, B. Gilomen, J. S. Siegel, *Org. Process Res. Dev.* **2012**, *16*, 664 – 676.
[4] X. Li, F. Kang, M. Inagaki, *Small* **2016**, *12*, 3206 – 3223.
[5] a) T. Janowski, P. Pulay, A. A. S. Karunarathna, A. Sygula, S. Saebo, *Chem. Phys. Lett.* **2011**, *512*, 155 – 160; b) P. A. Denis, *Chem. Phys. Lett.* **2011**, *516*, 82 – 87; c) Y. Zhao, D. G. Truhlar, *Phys. Chem. Chem. Phys.* **2008**, *10*, 2813 – 2818; d) E. A. Jackson, B. D. Steinberg, M. Bancu, A. Wakamiya, L. T. Scott, *J. Am. Chem. Soc.* **2007**, *129*, 484 – 485.
[6] L. N. Dawe, T. A. AlHujran, H. A. Tran, J. I. Mercer, E. A. Jackson, L. T. Scott, P. E. Georghiou, *Chem. Commun.* **2012**, *48*, 5563 – 5565.
[7] M. Yamada, K. Ohkubo, M. Shionoya, S. Fukuzumi, *J. Am. Chem. Soc.* **2014**, *136*, 13240 – 13248.
[8] A. Sygula, *Synlett* **2016**, *27*, 2070 – 2080.
[9] a) V. H. Le, M. Yanney, M. McGuire, A. Sygula, E. A. Lewis, *J. Phys. Chem. B* **2014**, *118*, 11956 – 11964; b) C. Mück-Lichtenfeld, S. Grimme, L. Kobryn, A. Sygula, *Phys. Chem. Chem. Phys.* **2010**, *12*, 7091 – 7097; c) A. Sygula, F. R. Fronczek, R. Sygula, P. W. Rabideau, M. M. Olmstead, *J. Am. Chem. Soc.* **2007**, *129*, 3842 – 3843; d) C. M. Álvarez, L. A. Garcia-Escudero, R. Garcia-Rodriguez, J. M. Martin-Alvarez, D. Miguel, V. M. Rayon, *Dalton Trans.* **2014**, *43*, 15693 – 15696; e) M. Yanney, F. R. Fronczek, A. Sygula, *Angew. Chem. Int. Ed.* **2015**, *54*, 11153 – 11156; *Angew. Chem.* **2015**, *127*, 11305 – 11308; f) M. Yanney, A. Sygula, *Tetrahedron Lett.* **2013**, *54*, 2604 – 2607; g) A. Sygula, M. Yanney, W. P. Henry, F. R. Fronczek, A. V. Zabula, M. A. Petrukhina, *Cryst. Growth Des.* **2014**, *14*, 2633 – 2639; h) C. M. Álvarez, G. Aullon, H. Barbero, L. A. Garcia-Escudero, C. Martinez-Perez, J. M. Martin-Alvarez, D. Miguel, *Org. Lett.* **2015**, *17*, 2578 – 2581.
[10] a) A. S. Filatov, L. T. Scott, M. A. Petrukhina, *Cryst. Growth Des.* **2010**, *10*, 4607 – 4621; b) B. D. Steinberg, E. A. Jackson, A. S. Filatov, A. Wakamiya, M. A. Petrukhina, L. T. Scott, *J. Am. Chem. Soc.* **2009**, *131*, 10537 – 10545.
[11] S. Lampart, L. M. Roch, A. K. Dutta, Y. Wang, R. Warshamanage, A. D. Finke, A. Linden, K. K. Baldridge, J. S. Siegel, *Angew. Chem. Int. Ed.* **2016**, *55*, 14648 – 14652; *Angew. Chem.* **2016**, *128*, 14868 – 14872.
[12] S. Mizyed, P. E. Georghiou, M. Bancu, B. Cuadra, A. K. Rai, P. C. Cheng, L. T. Scott, *J. Am. Chem. Soc.* **2001**, *123*, 12770 – 12774.
[13] a) S. Gonell, M. Poyatos, E. Peris, *Chem. Eur. J.* **2014**, *20*, 9716 – 9724; b) A. Prades, E. Peris, M. Alcarazo, *Organometallics* **2012**, *31*, 4623 – 4626; c) H. Valdés, M. Poyatos, E. Peris, *Organometallics* **2015**, *34*, 1725 – 1729; d) S. Gonell, M. Poyatos, E. Peris, *Angew. Chem. Int. Ed.* **2013**, *52*, 7009 – 7013; *Angew. Chem.* **2013**, *125*, 7147 – 7151.
[14] E. Peris, *Chem. Commun.* **2016**, *52*, 5777 – 5787.
[15] a) D. Brynn Hibbert, P. Thordarson, *Chem. Commun.* **2016**, *52*, 12792 – 12805; b) A. J. Lowe, F. M. Pfeffer, P. Thordarson, *Supramol. Chem.* **2012**, *24*, 585 – 594; c) P. Thordarson, *Chem. Soc. Rev.* **2011**, *40*, 1305 – 1323.
[16] a) E. Freire, O. L. Mayorga, M. Straume, *Anal. Chem.* **1990**, *62*, 950A – 959A; b) T. Wiseman, S. Williston, J. F. Brandts, L. N. Lin, *Anal. Biochem.* **1989**, *179*, 131 – 137.
[17] Gaussian 09, Revision D.01, M. J. Frisch, G. W. Trucks, H. B. Schlegel, G. E. Scuseria, M. A. Robb, J. R. Cheeseman, G. Scalmani, V. Barone, B. Mennucci, G. A. Petersson, H. Nakatsuji, M. Caricato, X. Li, H. P. Hratchian, A. F. Izmaylov, J. Bloino, G. Zheng, J. L. Sonnenberg, M. Hada, M. Ehara, K. Toyota, R. Fukuda, J. Hasegawa, M. Ishida, T. Nakajima, Y. Honda, O. Kitao, H. Nakai, T. Vreven, J. A. Montgomery, Jr., J. E. Peralta, F. Ogliaro, M. Bearpark, J. J. Heyd, E. Brothers, K. N. Kudin, V. N. Staroverov, R. Kobayashi, J. Normand, K. Raghavachari, A. Rendell, J. C. Burant, S. S. Iyengar, J. Tomasi, M. Cossi, N. Rega, J. M. Millam, M. Klene, J. E. Knox, J. B. Cross, V. Bakken, C. Adamo, J. Jaramillo, R. Gomperts, R. E. Stratmann, O. Yazyev, A. J. Austin, R. Cammi, C. Pomelli, J. W. Ochterski, R. L. Martin, K. Morokuma, V. G. Zakrzewski, G. A. Voth, P. Salvador, J. J. Dannenberg, S. Dapprich, A. D. Daniels, Ö. Farkas, J. B. Foresman, J. V. Ortiz, J. Cioslowski, D. J. Fox, Gaussian, Inc., Wallingford, CT, **2009**.

Manuscript received: April 18, 2017
Accepted manuscript online: May 26, 2017
Version of record online: July 13, 2017